

## **Appendix 6**

### **Mineralogical and geochemical alteration of the MX80 bentonite from the LOT experiment**

Kaufhold S., Dohrmann, R.

BGR Bundesanstalt für Geowissenschaften und Rohstoffe, LBEG Landesamt für Bergbau, Energie und Geologie, Stilleweg 2, D-30655 Hannover, Germany  
email of corresponding author: [s.kaufhold@bgr.de](mailto:s.kaufhold@bgr.de)

# Mineralogical and geochemical alteration of the MX80 bentonite from the LOT experiment –

## Characterization of the A2 parcel

Kaufhold S., Dohrmann, R.

BGR Bundesanstalt für Geowissenschaften und Rohstoffe, LBEG Landesamt für Bergbau, Energie und Geologie, Stilleweg 2, D-30655 Hannover, Germany  
email of corresponding author: s.kaufhold@bgr.de

### Abstract

Bentonites are believed to represent a suitable geotechnical barrier in HLRW repositories and, therefore, are investigated with respect to long term stability under the conditions expected. In order to identify the type and extend of possible bentonite alteration processes long term tests have to be performed. Particularly valuable information is gained from in-situ tests which are commonly conducted in underground rock laboratories (URL). The LOT test performed by SKB is one of the outstanding tests due to the long test period accounting for 6 years including 5 years heating period. In this study chemical and mineralogical alteration processes of the bentonite after the 5 years heating period are investigated.

By in-situ  $\mu$ -EDXRF an increased Cu concentration was detected at the surface and along a profile until a depth of ca. 2 cm. By standard bulk XRF a slightly increased Cu concentration was found even in 4 cm distance from the Cu tube. Surprisingly, Cu was not detected on the exchange sites of the smectite. Accordingly, Cu has to be present as a separate phase. On the surface of the bentonite sample which was in direct contact with the Cu tube a bluish phase with metallic glance was found by light microscopy. SEM-EDX proved the dominance of Cu and S within this phase. In addition, by thermal analysis in combination with evolved gas analysis (DTA-MS) the presence of Cu-sulphides within the first cm is indicated. This raises the question about the S source. In the bentonite applied (MX80 from Wyoming) S predominantly occurs as sulphate (gypsum). Alternatively S could stem from dissolved sulphate of the pore water which entered the system during the experiment. Regardless of the two possible S sources it can be concluded that Cu corrosion directly or indirectly led to sulphate reduction. Based on the available data it is impossible to decide whether  $\text{SO}_4$  from the external water or from the gypsum of the bentonite was reduced by Cu corrosion. It can be concluded - regardless of this open question – that the selection of a bentonite being poor in  $\text{SO}_4$  (not containing sulphides or sulphates) would lead to reduction of the corrosion rate.

Parallel studies conducted by SKB, ONDRAF, and NAGRA proved the redistribution of water extractable  $\text{SO}_4$  over the entire bentonite block distance (10 cm). Surprisingly, a  $\text{SO}_4$  depletion was found both in the inner part (contact to Cu tube) and in the outermost 5 cm. On the other hand, a  $\text{SO}_4$  peak was found at appr. 3 cm distance from the heater. During the experiment water flew at the inner and outer surface of the bentonite block. Hence it is conceivable that this water dissolved the partially soluble gypsum which has been homogeneously distributed over the 10 cm of the bentonite block as the experiment started. Such dissolution – precipitation processes conceivably affect porosity and in turn the hydraulic conductivity.

Therefore, the selection of a bentonite being poor in partly soluble minerals as calcite or gypsum would help to reduce the extend of dissolution – precipitation processes. No unambiguous evidence for (structural) alteration of the montmorillonite was found. However, a slight increase of Mg nearby the heater could be detected indicating that some Mg was released from the montmorillonite. Interestingly, this result corresponds to the results obtained from the Mont Terri Heater project (Plötze et al., 2007). It is concluded that Mg release occurred to such a small extend that structural changes (e.g. change of layer charge density) could not be detected by IR, XRD, CEC and Alkylammoniummethod.

## **Introduction**

Bentonite is a candidate material as geotechnical barrier in high level radioactive waste (HLRW) repositories. However, one important open question with respect to safety assessment of the whole system is the long term stability. Bentonite properties are known to be affected by high pH solutions (e.g. cement pore water), highly saline waters, and by extensive drying. In this context illitization and / or the irreversible collapse of smectitic layers are particularly considered. Long term tests have to be performed in order to identify such processes and to learn more about the stability of bentonites under the conditions expected in a HLRW repository. However, bentonite cannot be considered as instable material even though different bentonite alteration processes are known. Therefore, either exaggerated conditions or a long time period have to be applied. Exaggerated conditions might lead to alteration processes which would not occur under realistic conditions. Therefore, performing long term tests covering a significant period of time are particularly valuable for bentonite research. In this respect, the LOT test as conducted by SKB represents a currently outstanding in-situ test. Detailed information about this test is given by Karnland et al. (2000). In this paper the mineralogical and chemical alteration processes which occurred within the first 5 – 6 years (5 years heating) are investigated.

## Materials & methods

In the LOT experiment conducted by SKB, different scenarios were included in the experimental setup. As an example, Cu plates were inserted as well as potassium feldspar. Therefore, the exact location of investigated samples has to be known in order to ensure comparability of results obtained by different laboratories.

BGR received a sample from the extensively heated part (15) of the A2 parcel. The experimental setup, temperature distribution at equilibrium conditions, and a photograph of the investigated sample are shown in Figure 1.

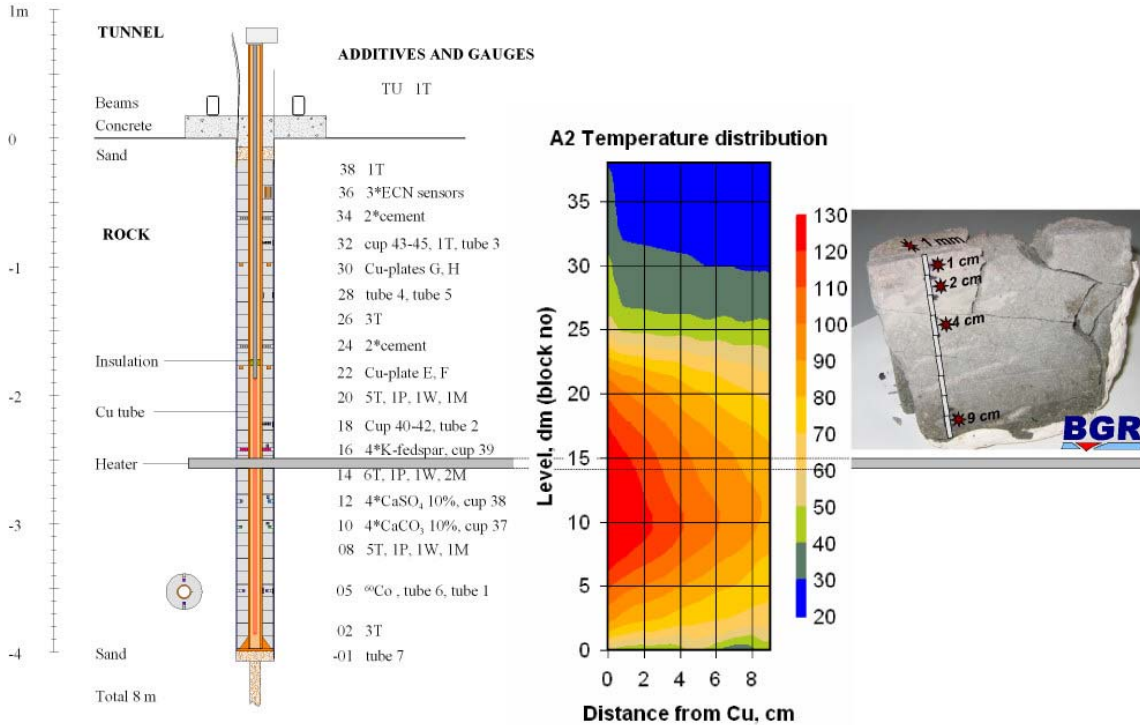


**Figure 1: Experimental setup, temperature distribution at equilibrium conditions (source: SKB). The sampling of the slice of block 15 sent to BGR is shown in the photograph.**

The analyses conducted by BGR focused on mineralogical and chemical processes at the Cu - bentonite interface. This was thought to be most interesting since Cu corrosion was already evident from the macroscopic inspection of the Cu tube. It was decided to first continuously measure the Cu distribution by in-situ  $\mu$ -EDXRF.

During the LOT experiment the bentonite has been in contact with excess water which led to the slow but steady increase of swelling pressure in turn indicating ongoing water saturation. The water content of the sample, therefore, was comparably high and the tendency to release water at ambient laboratory conditions was obvious. For  $\mu$ -EDXRF analysis the block, except for the profile, was protected with plastic foil in order to prevent the slice from falling apart. This protection was sufficient to measure two replicates. Thereafter, the block was sampled (appr. 5 g / sample) according to Figure 1. The sample called '1<sup>st</sup> mm' was collected by scraping off ca. 2 g from the very surface. The samples were dried at 60°C until constancy of weight and subsequently ground by a laboratory mortar mill.

The **in-situ- $\mu$ EDXRF** measurements were performed by the combination of an ITRAX microscope and a geoscanner, as it is distributed by COX analytical systems. The chemical composition was determined by **XRF** using a PANalytical Axios and a PW2400 XRF spectrometer.

For **XRD** analysis oriented mounts were produced by suction of a suspension (60 mg of clay dispersed in 2 ml of deionised water) through porous ceramic plates. XRD pattern were recorded on a Seifert 3003 TT diffractometer, using  $\text{CuK}\alpha$  radiation before and after exposure to an ethyleneglycol atmosphere.

The cation exchange capacity was determined by the **BaCl<sub>2</sub>** method according to MEHLICH (1948) but without buffering and using a batch technique instead of percolation.

For recording mid **infrared** (MIR) spectra the KBr pellet technique (1 mg sample / 200 mg KBr) was applied. Spectra were collected on a Thermo Nicolet Nexus FTIR spectrometer (beam splitter: KBr, detector DTGS TEC).

Near infrared (NIR) spectra were recorded using the DRIFT-technique, beam splitter  $\text{CaF}_2$ , detector InGaS. Both MIR and NIR spectra consist of 32 scans each. The resolution was adjusted to  $2\text{ cm}^{-1}$ .

**Thermoanalytical** investigations were performed by a Netzsch 409 PC thermobalance equipped with a DSC/TG sample holder linked to a Balzers Thermostar quadrupole mass spectrometer (MS). 100 mg of powdered material previously equilibrated at 53 % r.H. is heated from 25 -1000°C with a heating rate of 10 K/min.

Scanning electron microscopy (**SEM**) was performed on an ESEM (environmental scanning electron microscope) from FEI Quanta 600 FEG.

The specific surface area (**SSA**) was determined by  $\text{N}_2$  adsorption using a 5 point BET method. Measurements were performed by a Micromeritics Gemini III 2375 surface area analyzer with ca. 300 mg weight.

The **water uptake capacity** was determined gravimetrically. Defined temperature and humidity were provided by a climate oven. Approximately 0.5 g sample was weighed in an Al crucible and equilibrated at 50, 60, and 70 % RH for one week each.

The layer charge density (**LCD**) was determined by the alkylammonium method (Lagaly, 1994). Lagaly proposed to use a set of n-alkylammonium ions ( $n_c = 6 - 18$ ) which provides information about layer charge density distribution. However, in some cases only a value for the mean layer charge density is desired. Accordingly, Olis et al. (1990) suggested using the dodecylammonium ion, only. In this study we applied chain lengths 11, 12, and 13, in order to increase statistical significance. For the calculation of LCD values from the different d-spacing own unpublished calibrations were used. These calibrations were established by considering 13 different bentonites which covered a LCD range from 0.30 to 0.35 eq/FU.

## Results and discussion

### XRF

Chemical analyses based on XRF, in contrast to common quantitative mineralogical methods, provide precise values indirectly reflecting the mineralogical composition. These values are very useful for the identification of mineral alteration processes. Particularly relative differences are considered to be mineralogically meaningful even within the 1 % range. The chemical composition as determined by XRF of all samples is given in Table 1.

**Table 1: Major element composition (XRF) normalized to LOI = 0 (LOI values given separately).**

		1 mm	1 cm	2 cm	4 cm	9 cm
		1 <sup>st</sup> block	1 <sup>st</sup> block	1 <sup>st</sup> block	1 <sup>st</sup> block	1 <sup>st</sup> block
SiO <sub>2</sub>	[wt.-%]	68.3	68.3	68.3	67.7	68.4
TiO <sub>2</sub>	[wt.-%]	0.2	0.2	0.2	0.2	0.2
Al <sub>2</sub> O <sub>3</sub>	[wt.-%]	20.7	20.8	20.7	20.5	20.7
Fe <sub>2</sub> O <sub>3</sub>	[wt.-%]	3.9	4.0	4.0	4.0	4.0
MnO	[wt.-%]	0.0	0.0	0.0	0.0	0.0
MgO	[wt.-%]	3.0	2.7	2.7	2.5	2.4
CaO	[wt.-%]	1.2	1.2	1.3	1.8	1.3
Na <sub>2</sub> O	[wt.-%]	2.0	2.0	2.0	2.1	2.1
K <sub>2</sub> O	[wt.-%]	0.5	0.5	0.5	0.5	0.5
P <sub>2</sub> O <sub>5</sub>	[wt.-%]	0.1	0.1	0.0	0.0	0.1
(SO <sub>3</sub> )	[wt.-%]	0.2	0.2	0.3	0.7	0.3
(Cl)	[wt.-%]	0.0	0.0	0.0	0.0	0.0
(F)	[wt.-%]	<0.05	<0.05	<0.05	<0.05	0.06
Sum	[wt.-%]	100.0	100.0	100.0	100.0	100.0
LOI	[wt.-%]	11.1	10.4	10.1	10.1	9.2

The sample from the first mm, in contrast to samples 1 – 4 cm, reveals an appr. 1 % higher loss on ignition (LOI) whereas the LOI of the sample at 9 cm is appr. 1 % lower. This affects XRF values of all elements/oxides and in turn pretends meaningless trends. One example is given in Figure 2. To avoid this misinterpretation in the following only values which were normalized to LOI = 0 are considered.

Using these corrected data in case of SiO<sub>2</sub> and Al<sub>2</sub>O<sub>3</sub> slightly lower values of 'sample 4 cm' were observed (Figure 3). No systematic deviation of the Fe<sub>2</sub>O<sub>3</sub> content could be observed. In contrast, the MgO content increased nearby the Cu tube (Figure 4). Figure 5 shows a CaO and SO<sub>3</sub> peak at 4 cm which cannot be attributed to material heterogeneity which was proved before the experiment to be significantly lower. It is tentatively concluded that gypsum redistributed during the 5 (6) years of the project. Other studies conducted by Andra, SKB (a.o.; yet unpublished) report a maximum gypsum concentration at 3 cm. However, in this study no sample was collected at this depth. In conclusion, the maximum gypsum concentration at 4 cm observed in this study probably represents the right shoulder of the actual peak.

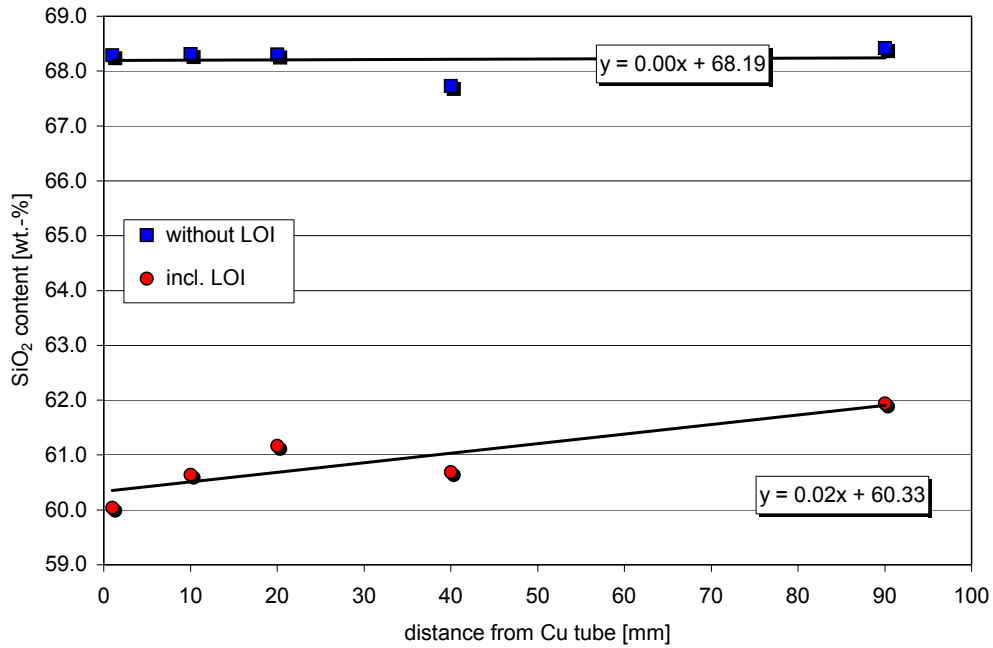


Figure 2: comparison of SiO<sub>2</sub> content before and after correction of XRF data for the loss on ignition (LOI).

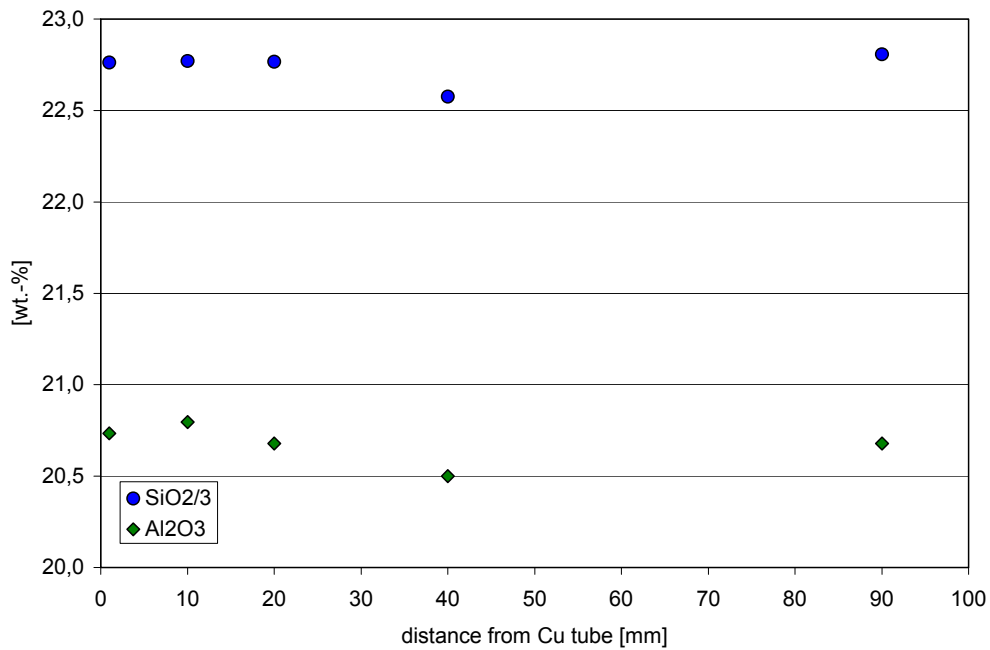


Figure 3: Al<sub>2</sub>O<sub>3</sub> and SiO<sub>2</sub> content (SiO<sub>2</sub> content is divided by 3) depending on the distance from the Cu tube.

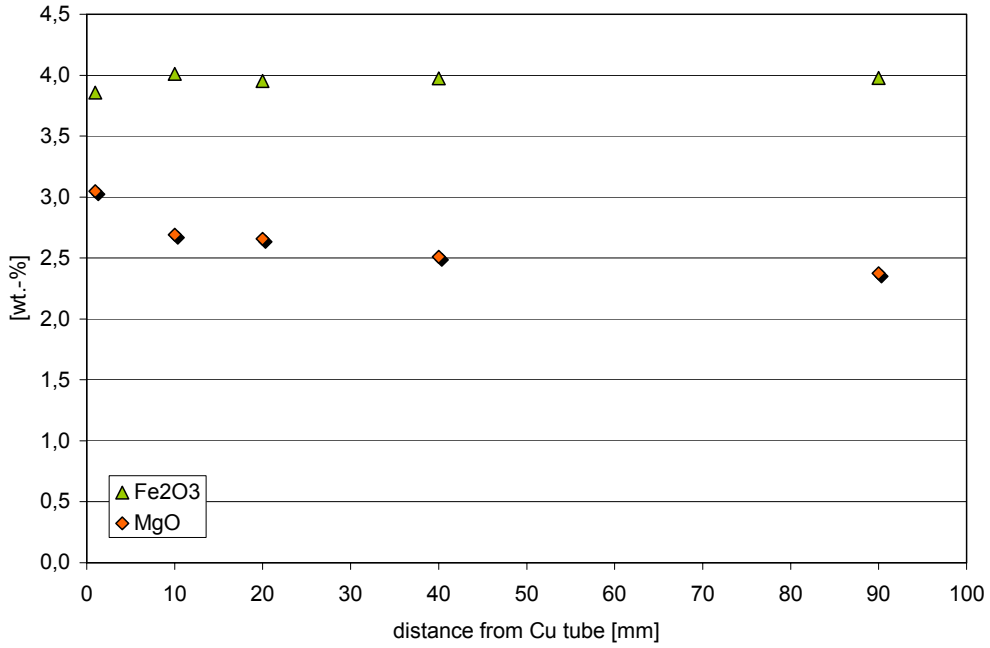


Figure 4: MgO and Fe<sub>2</sub>O<sub>3</sub> content depending on the distance from the Cu tube.

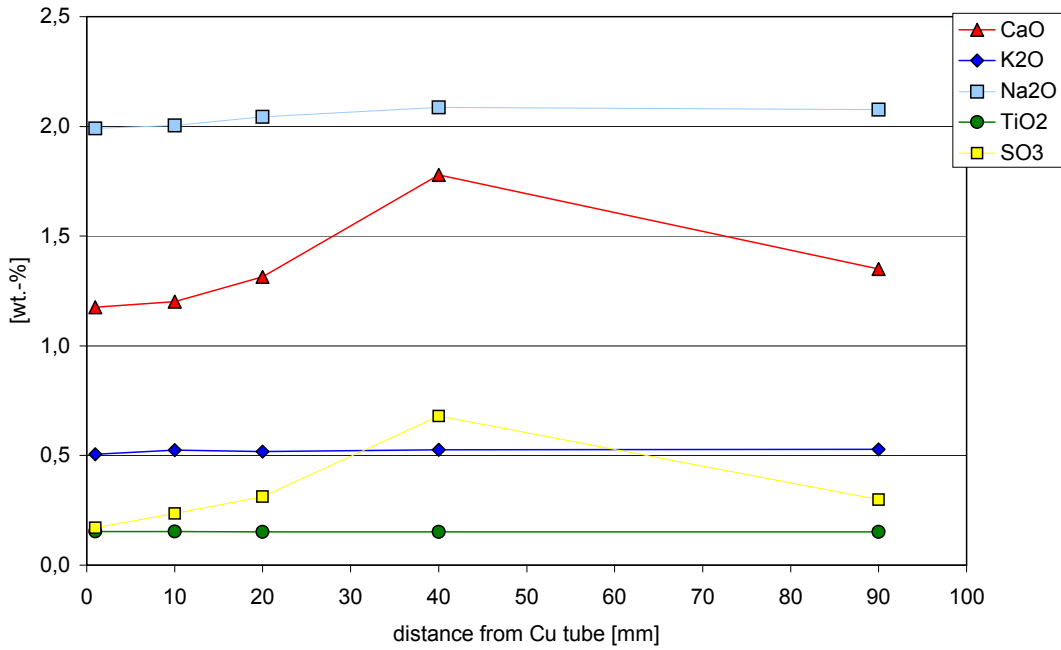


Figure 5: CaO, K<sub>2</sub>O, Na<sub>2</sub>O, TiO<sub>2</sub>, and SO<sub>3</sub> (XRF) content depending on the distance from the Cu tube.

**Table 2: Trace element composition (XRF).**

		mm 1	mm 10	mm 20	mm 40	mm 90
As	[mg/kg]	13	14	11	11	13
Ba	[mg/kg]	<b>177</b>	<b>215</b>	<b>328</b>	<b>331</b>	<b>271</b>
Bi	[mg/kg]	<3	<3	<3	<3	<3
Ce	[mg/kg]	104	112	111	116	116
Co	[mg/kg]	<3	<3	<3	<3	<3
Cr	[mg/kg]	11	60	27	72	10
Cs	[mg/kg]	<5	<5	<5	<5	<5
Cu	[mg/kg]	<b>5764</b>	<b>4075</b>	<b>240</b>	<b>50</b>	<b>&lt;10</b>
Ga	[mg/kg]	26	27	27	27	28
Hf	[mg/kg]	8	5	8	7	7
La	[mg/kg]	38	32	32	31	38
Mo	[mg/kg]	<b>27</b>	<b>6</b>	<b>&lt;2</b>	<b>3</b>	<b>3</b>
Nb	[mg/kg]	27	26	27	30	27
Nd	[mg/kg]	<50	<50	55	<50	<50
Ni	[mg/kg]	<b>&lt;3</b>	5	<3	<3	<3
Pb	[mg/kg]	27	32	44	46	42
Rb	[mg/kg]	10	12	9	10	10
Sb	[mg/kg]	<5	<5	<5	5	<5
Sc	[mg/kg]	5	5	5	5	6
Sm	[mg/kg]	<50	<50	<50	<50	<50
Sn	[mg/kg]	9	11	8	9	7
Sr	[mg/kg]	213	220	233	301	215
Ta	[mg/kg]	10	7	<5	7	<5
Th	[mg/kg]	45	41	43	41	43
U	[mg/kg]	18	15	20	17	20
V	[mg/kg]	9	<5	<5	7	10
W	[mg/kg]	<5	<5	<5	<5	<5
Y	[mg/kg]	37	39	39	37	38
Zn	[mg/kg]	93	59	125	109	101
Zr	[mg/kg]	179	184	175	181	181

With respect to the trace element composition three significant systematic variations were observed.

First of all a surprisingly high content of Cu was found even within the 1<sup>st</sup> cm indicating that Cu corrosion a) occurred and b) led to penetration of Cu into the bentonite. Even the 50 mg/kg which were observed in the '40 mm sample' likely result from Cu migration (Wyoming bentonites commonly are poor in Cu).

The high Mo content in 'sample 1 mm' is supposed to also result from tube corrosion. A third effect was found for Ba displaying the same trend as was found for gypsum (CaO and SO<sub>3</sub>). This can be explained either by gypsum containing small amounts of Ba or by the presence of traces of baryte being present already in the precursor material.

In summary,

- a) an increased Cu and Mo content even in 2 cm distance,
- b) a CaO, Ba, and SO<sub>3</sub> peak at appr. 40 mm, and
- c) a higher MgO content nearby the Cu tube was found.

In conclusion, a) indicates corrosion, b) indicates sulphate redistribution, and c) raises the suspicion that something happened to the montmorillonite (cation exchange or structural alteration).

### ***In-situ $\mu$ -EDXRF***

The in-situ  $\mu$ -EDXRF as applied provides continuous but only relative intensity information. Therefore, the curves were roughly fitted to the XRF Cu values. The quality of calibration does not allow for the accurate interpretation of  $\mu$ -EDXRF data. However, it could be clearly proved that Cu penetrated the clay until a depth of 2 – 2.5 cm. From Figure 6 it is evident that bulk XRF data were confirmed with respect to Cu penetration depths.

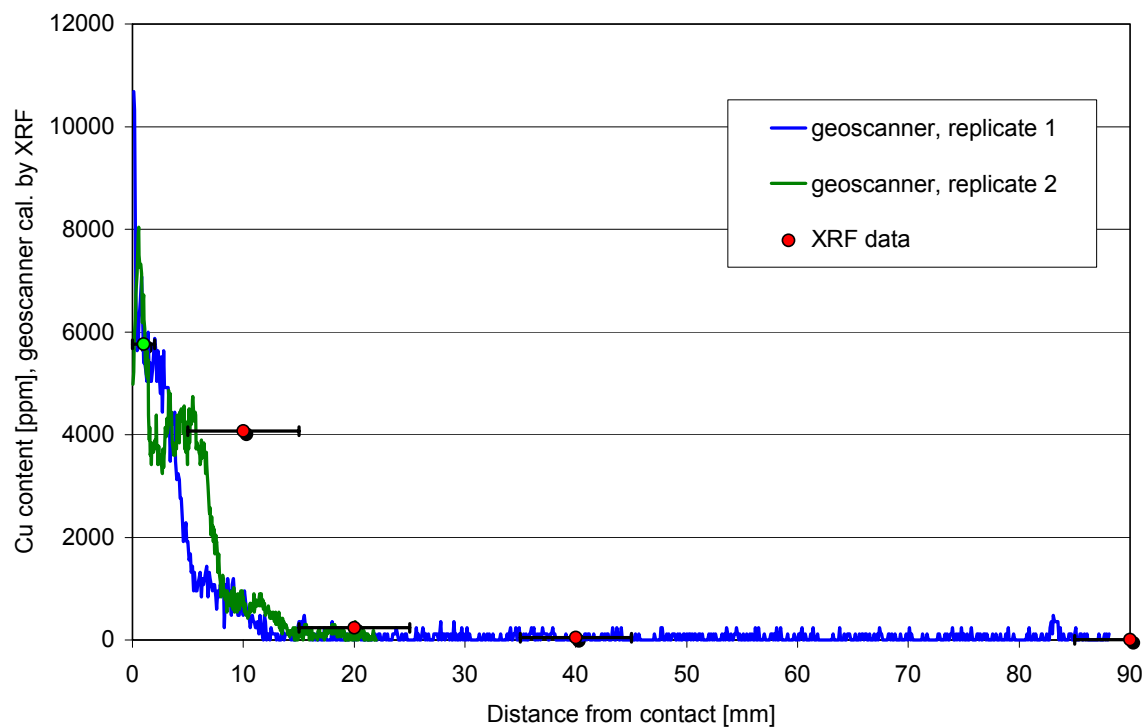


**Figure 6: in-situ  $\mu$ -EDXRF investigation of Cu-concentration of LOT bentonite block A2 (15).**

In addition the Fe concentration was measured by in-situ  $\mu$ -EDXRF. No systematic Fe redistribution could be detected (Figure 7).

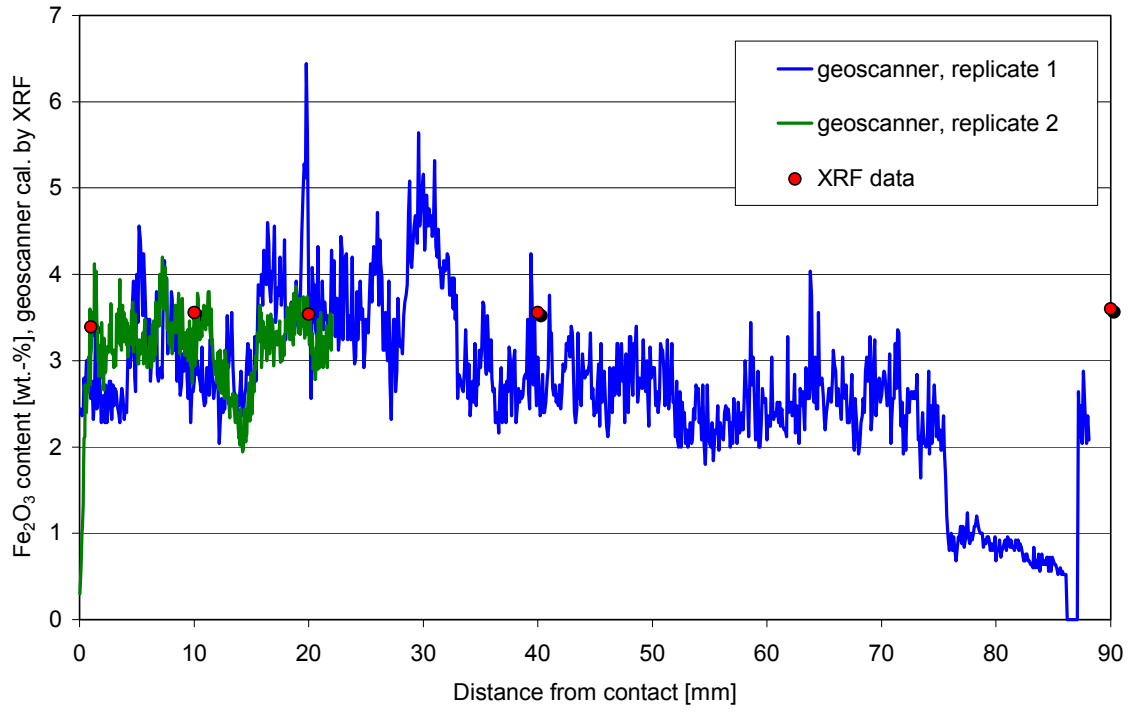


Figure 7: In-situ  $\mu$ -EDXRF investigation of Cu-concentration of LOT bentonite block A2 (15).

## XRD

By XRD a trace of gypsum was found in the 4 cm sample (Figure 8) which confirms the trend observed by XRF (Figure 5). In addition a slightly more distinct and relatively sharp illite 001 reflection was found in sample 4 cm likely indicating material heterogeneity or texture effect. Small differences of the 001 reflection of the dried material can be attributed to varying (re-)hydration state. The differences in peak positions of the first and second order of the basal reflections observed after EG solvation are relatively small and hence do not allow to suppose structural changes. The intensity differences are quite large. However, this is assumed to stem from typical problems with sample preparation of these clays.

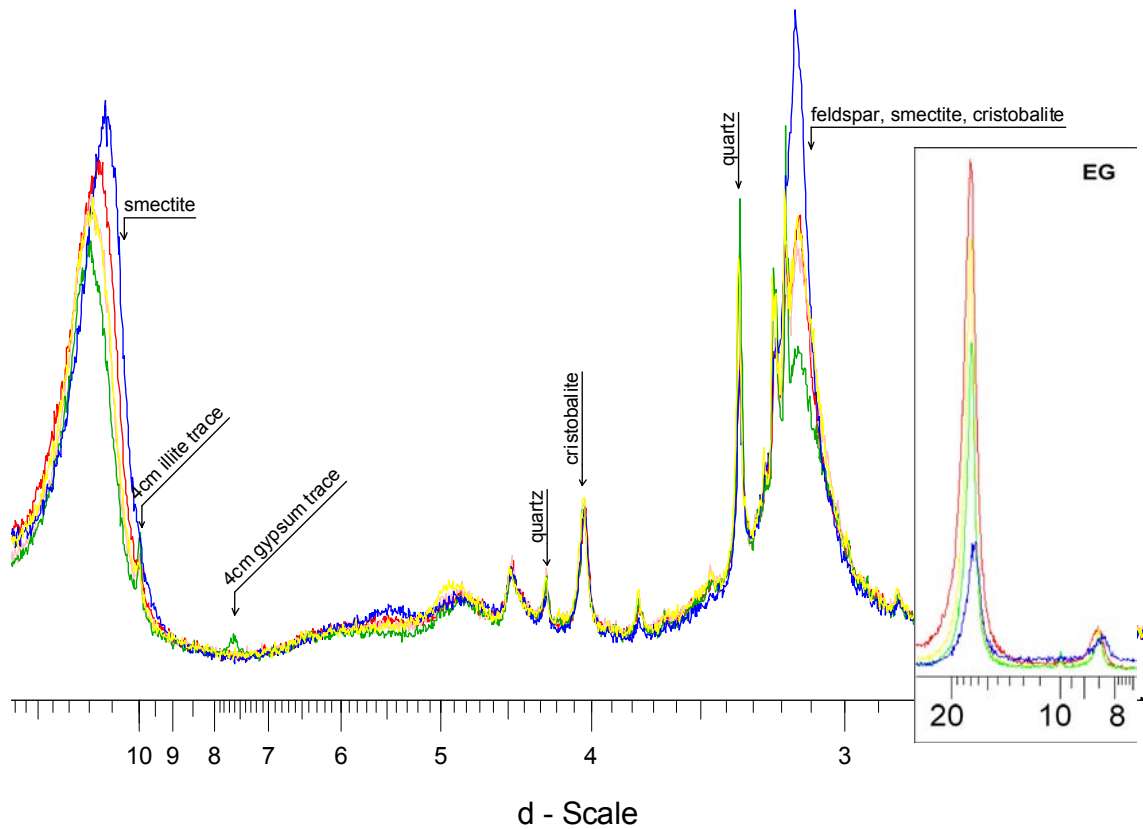


Figure 8: XRD pattern of oriented mounts dried at 60°C and 001 and 002 reflection of EG saturated material (red = 1 mm, orange = 1 cm, yellow = 2 cm, green = 4 cm, blue = 9 cm).

## CEC

At the BGR clay laboratory commonly the Cu triene method is used for CEC determination. In this study the BaCl<sub>2</sub> method was selected since Cu was believed to play an important role and triethylenetetramine as strong complexing agent for Cu could facilitate dissolution of possible Cu corrosion products. With respect to the present study it is important to note that the BaCl<sub>2</sub> requires the repeated addition of different solutions which leads to the extensive dissolution of relatively soluble mineral phases as calcite or gypsum. The specific problems of this method are discussed in detail by Dohrmann (2006). However, in the present study the CEC method was mainly conducted in order to a) identify the fate of Cu released from the tube by corrosion (did it exchange for Na<sup>+</sup> ?) and b) identify possible montmorillonite alterations.

For answering these questions the BaCl<sub>2</sub> method was thought to be applicable (results are presented in Table 3).

**Table 3: Exchangeable cations (including Cu), sum of cations and total Ba<sup>2+</sup> which was exchanged representing CEC (BaCl<sub>2</sub> method). Average values of different initial weights of samples (0.300 and 0.500 g).**

sample	K <sup>+</sup> [meq/100g]	Na <sup>+</sup> [meq/100g]	Ca <sup>2+</sup> [meq/100g]	Mg <sup>2+</sup> [meq/100g]	Cu <sup>2+</sup> [meq/100g]	sum cations [meq/100g]	Ba <sup>2+</sup> [meq/100g]
1 mm	2,5	60,4	28,6	11,9	0,0	103,4	87,5
1 cm	1,7	63,2	28,5	11,7	0,1	105,2	86,5
2 cm	1,5	60,6	28,6	11,2	0,0	101,9	85,5
4 cm	1,2	59,0	32,3	11,0	0,0	103,5	80,5
9 cm	1,5	60,0	29,1	10,1	0,0	100,7	86,0

The sum of exchangeable cations, expectedly exceeds the CEC („Ba<sup>2+</sup>“) by 15 – 20 meq/100 g. This difference can be explained by dissolution of gypsum in the exchange solutions applied. We used different initial weights (0.300 and 0.500 g) in order to find out, if the total fraction of gypsum was dissolved. In case of presence of gypsum or calcite higher Ca<sup>2+</sup> values are obtained for the lower initial weight (Dohrmann 2006). In the present study no such dependence was observed which clearly indicates the complete dissolution of gypsum throughout the CEC experiment. In Figure 9 the maximum of the concentration of exchangeable Ca<sup>2+</sup> should correspond to the increase in CaO (XRF data, Figure 5). The increase of appr. 3.5 meq/100 g as observed in ‘sample 4 cm’ corresponds to appr. 0.3 wt.% gypsum or 0.1 wt.% CaO. In contrast, by XRF (Table 1) an increase of 0.5 wt.% CaO was found. This indicates the presence of an additional Ca-phase being less soluble than gypsum.

In addition, by XRF an increased MgO content was found near to the Cu tube. This result, qualitatively, could be confirmed by the exchangeable Mg analysis (Fig. 9) which increased by appr. 1 meq/100 g. However, by XRF a difference of appr. 0.4 wt.% was observed which, theoretically, would correspond to 5 meq/100 g. Therefore, the slight increase of exchangeable Mg is not sufficient to explain the total increase of MgO near to the Cu tube. It can be concluded that the additional Mg either occurs in newly precipitated hardly soluble phases or in the montmorillonites’ structure.

Generally, it is questionable whether such small XRF and CEC differences should be considered quantitatively. However, the results presented above should be kept in mind when investigating the LOT A3 parcel.

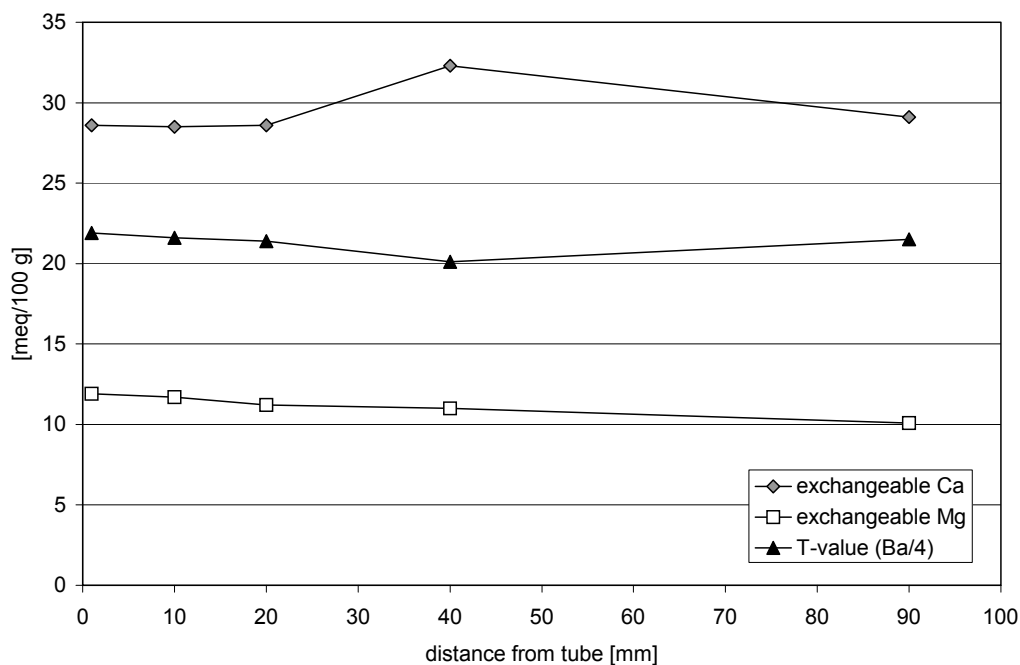


**Figure 9: Distribution of exchangeable  $\text{Ca}^{2+}$ ,  $\text{Mg}^{2+}$ , and  $\text{Ba}^{2+}$  (divided by 4), the latter representing the CEC.**

In Table 3 a slightly higher content of exchangeable  $\text{K}^+$  was found in the 1 mm sample. It is at least conceivable that  $\text{K}^+$  was adsorbed from the water at the Cu - bentonite interface.

CEC methods are sensitive towards changes of charges commonly caused by structural alterations. As can be seen in Figure 9 only the '4 cm sample' has a slightly lower CEC than the others. This cannot be explained only by the slightly lower montmorillonite content (due to higher gypsum / montmorillonite ratio; see chapter XRF). In addition, the CEC is known to be influenced by the pH value of the suspensions during cation exchange. However the slightly lower pH value of the '4 cm sample' (pH 9.7) compared to the others (pH 9.9) is not supposed to influence the CEC by more than 1 meq/100g. Accordingly, the lower CEC value of the '4 cm sample' can not be explained unambiguously.

Despite the different CEC value of the 4 cm sample no montmorillonite alteration processes nearby the Cu tube can be deduced from the CEC values of the '1 mm' and '1 cm' sample.

## DTA

Differential thermal analysis represents a suitable complementary analytical tool for the identification of specific minerals, especially if the gases evolved are characterized either by infrared spectroscopy or mass spectrometry. The differential scanning calorimetry curves of the BGR LOT samples is given in Figure 10. The corresponding mass spectrometer curves (mass 64) are given in Figure 11. All samples show the typical dehydration, dehydroxylation, and recrystallization reactions of smectites and the other minerals of MX 80 bentonite. In addition all curves show distinct peaks at ca. 900°C. These peaks can be assigned to the SO<sub>2</sub> release from gypsum and hence are clearly visible in the MS 64 curve (Figure 11).

The samples '1 mm' and '1 cm' in contrast to the others, exhibit one distinct peak at appr. 360°C. This peak was clearly observed in the MS curve indicating the presence of a S phase. According to Maurel (1964) this peak could represent the presence of covellite (CuS) or a related phase. This indicates that the corrosion product is a sulphide. The '1 cm sample', in contrast to the '1 mm sample', shows an additional peak at appr. 400°C indicating the presence of an additional phase in 1 cm depths. From the oxidation zones in Cu porphyry ore deposits it is known that a number of different CuS<sub>x</sub> phases exist varying in the Cu:S ratio depending on the geochemical milieu. The existence of different CuS<sub>(x)</sub> phases depending on the distance from the heater, therefore, is possible.

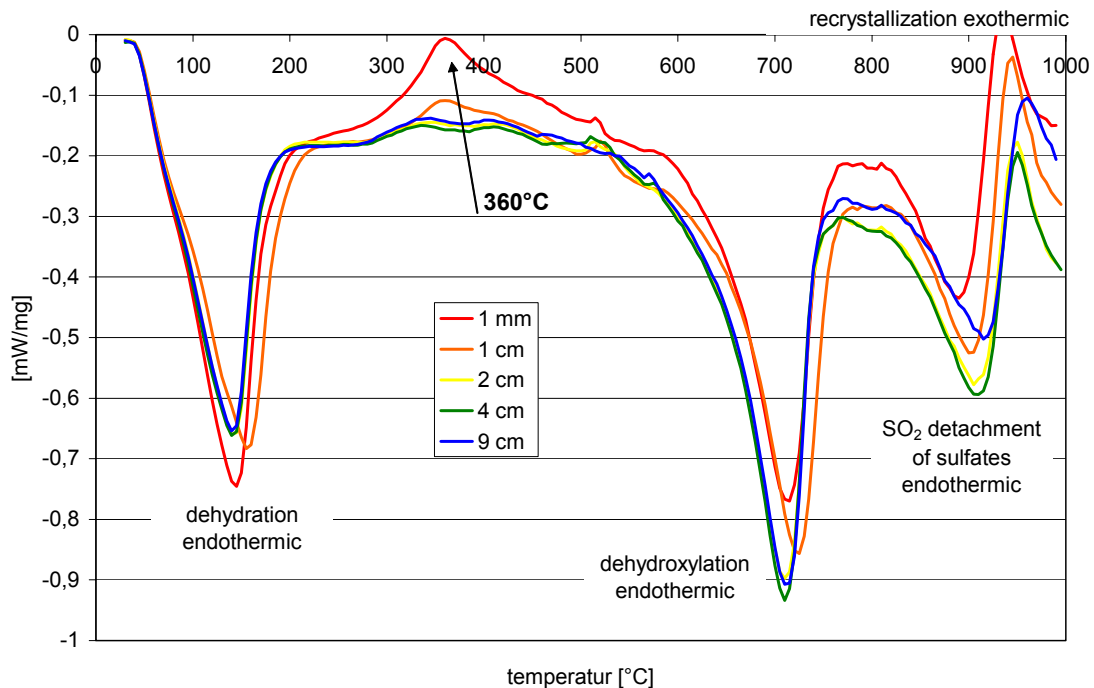


Figure 10: Differential scanning calorimetry (DSC) curves of all samples.

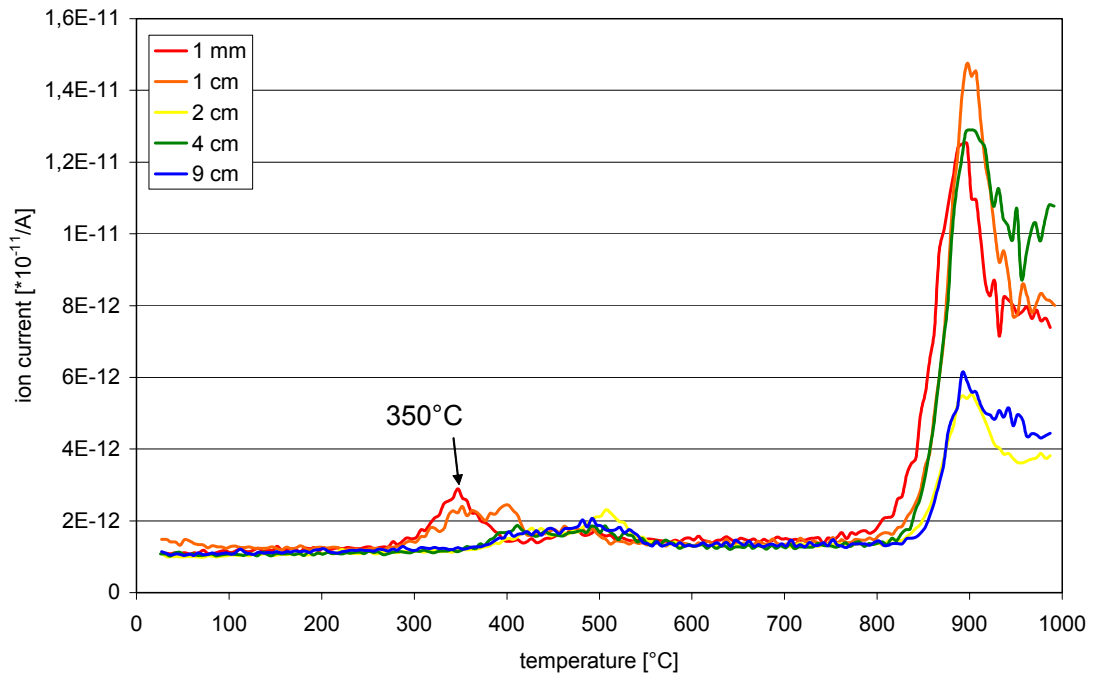


Figure 11: Mass spectrometer curves (mass 64) of all samples.

## IR

By infrared spectroscopy information about both the composition of smectites and the presence of some minor constituents can be gained. The most interesting MIR spectral range is shown in Figure 12. In the '9 cm sample' traces of carbonate were found either representing material heterogeneity or carbonate from the outside water. From XRF and CEC data the presence of gypsum was concluded. In the MIR spectra the main gypsum ( $\text{SO}_4$ ) vibration at ca.  $1145 \text{ cm}^{-1}$  could not be observed. However, very small bands at  $680$  and  $600 \text{ cm}^{-1}$ , which were particularly observed in the '4 cm sample', likely indicate the higher gypsum content in the '4 cm sample' compared to the others. Additionally, the presence of cristobalite and quartz as already found by XRD was confirmed. Considering the structural OH groups of the smectite (montmorillonite) no alterations could be detected. It is worth mentioning that changes in the %-range of the discussed minerals can not be identified by this method.

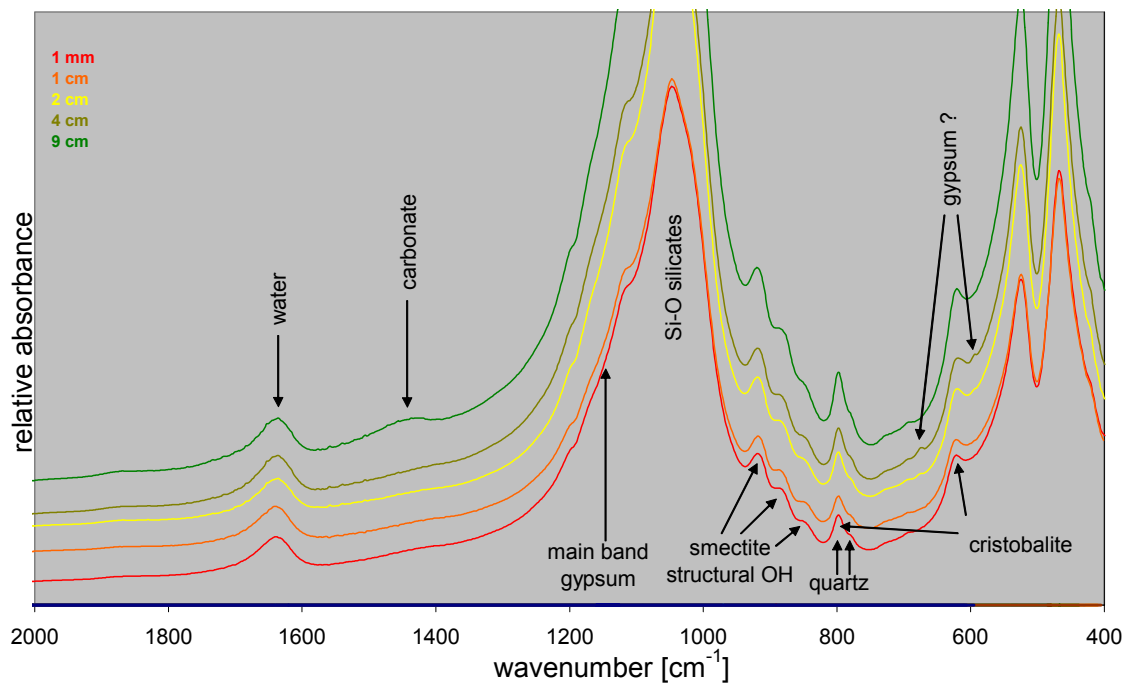
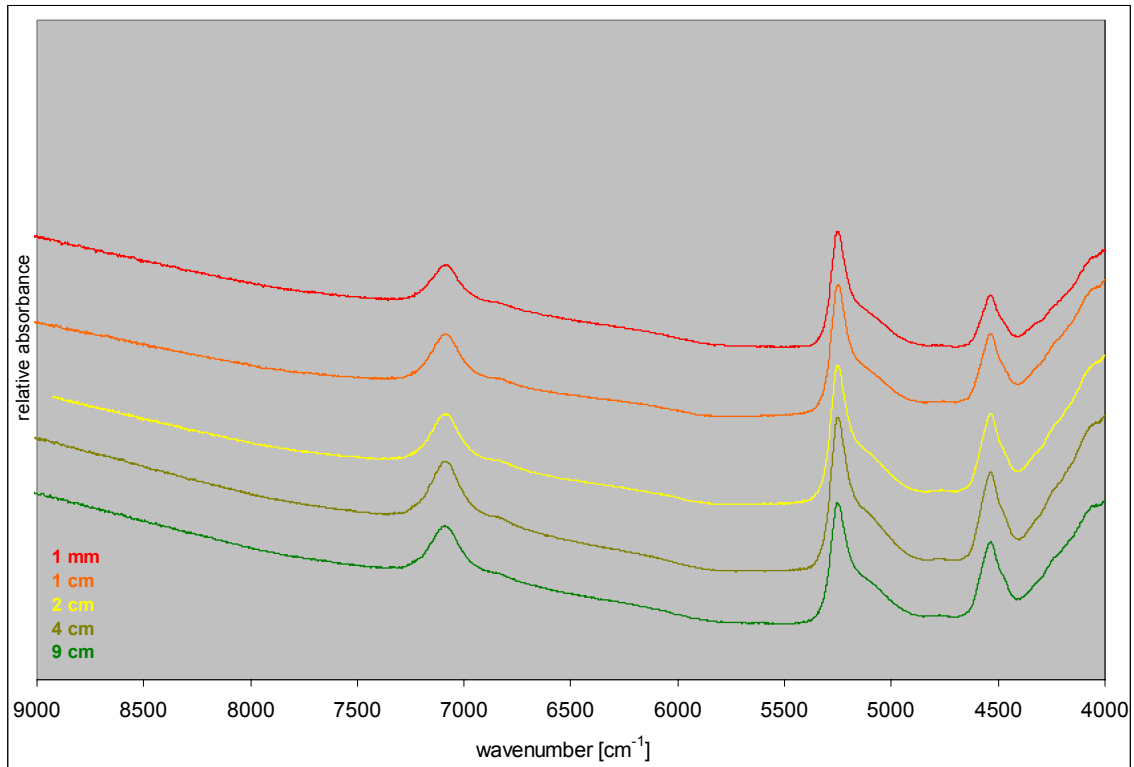


Figure 12: MIR spectra ( $400 - 2000 \text{ cm}^{-1}$ ) of all samples.



**Figure 13: NIR spectra of all samples.**

NIR spectra were collected to complement to CEC results. This is possible because the NIR band at  $5025\text{ cm}^{-1}$  (+  $5100\text{sh cm}^{-1}$ ) is sensitive to the type of cation (mono or divalent). As can be seen in Figure 13 no significant differences of the NIR spectra and particularly of the  $5025\text{ cm}^{-1}$  band could be observed.

## **BET**

Alteration processes including dissolution and precipitation may influence the specific surface area (SSA) which in case of bentonites mainly results from microporosity. It is at least conceivable that dissolution of specific mineral constituents leads to deblocking of pores and hence to an increase of SSA. Mineral precipitation, in turn, may lead to a decrease of SSA.

This theoretical process would explain the observed SSA distribution (Figure 14) showing a SSA minimum between 2 – 4 cm. In this distance a higher gypsum concentration was found possibly indicating precipitation of gypsum.

Based on the model explained above it is at least conceivable that the SSA values reflect gypsum redistribution.

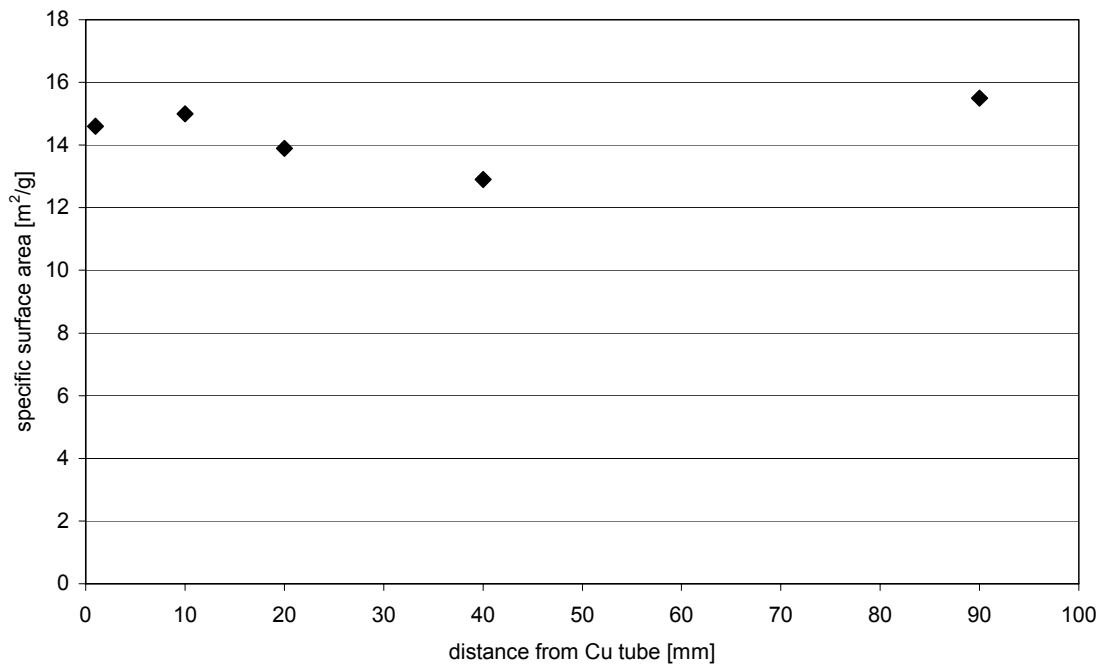


**Figure 14: specific surface area (from N<sub>2</sub> adsorption according to BET method)**

## ***Light and electron microscopy***

The surface of the bentonite block which has been in direct contact to the Cu tube was investigated by light microscopy. Clearly a bluish phase distinctly showing metallic glance could be observed (Figure 15). This grain was investigated by SEM (Figure 16).



**Figure 15: Light microscopy image of the bentonite - Cu tube contact surface (image width appr. 4 cm).**

By EDX the dominance of Cu and S of this grain was measured indicating that it is either a Cu sulphide or sulphate. The brightness of this grain is striking and results from high electrical conductivity being typical for metals and metal sulphides or oxides. This, together with the metallic glance observed by light microscopy, strongly indicates the presence of Cu sulphides rather than sulphates. Furthermore, small idiomorphic calcite crystals could be identified in the vicinity of the Cu sulphide grain (white arrow in Figure 16). In Figure 17 an example for the systematic EDX investigation of the bentonite sample is presented. In this figure small Cu sulphide particles as well as freshly appearing calcite grains could be identified by the qualitative elemental composition. However, the EDX spectra are affected by the underlying smectites which is caused by the small grain size of the calcite and the Cu sulphides ('matrix effect'). Hence, the structural elements, mainly Si and Al, can be observed in all spectra.

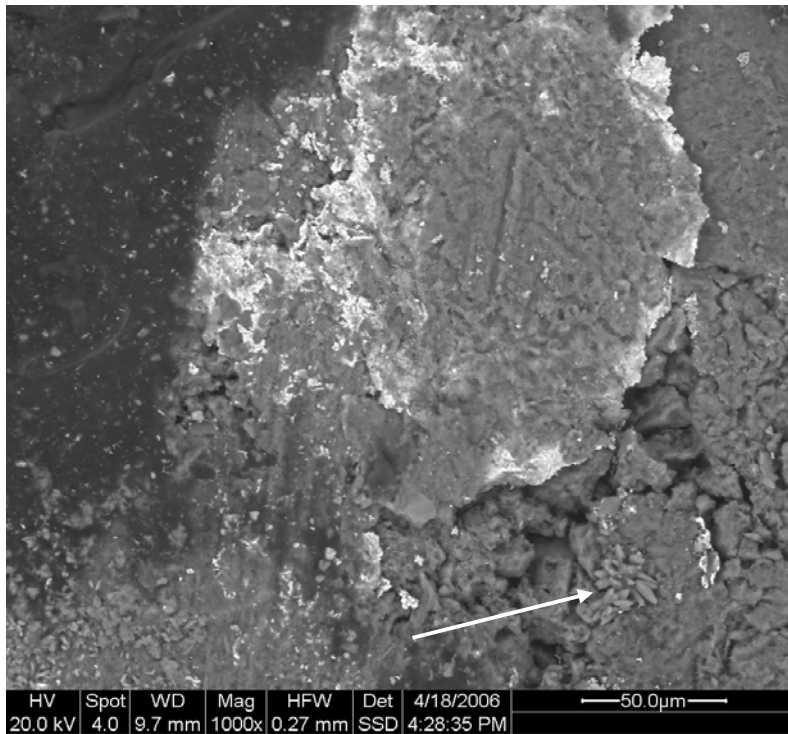


Figure 16: Electron microscopy image of the bluish metallic phase primarily identified in the light microscope.

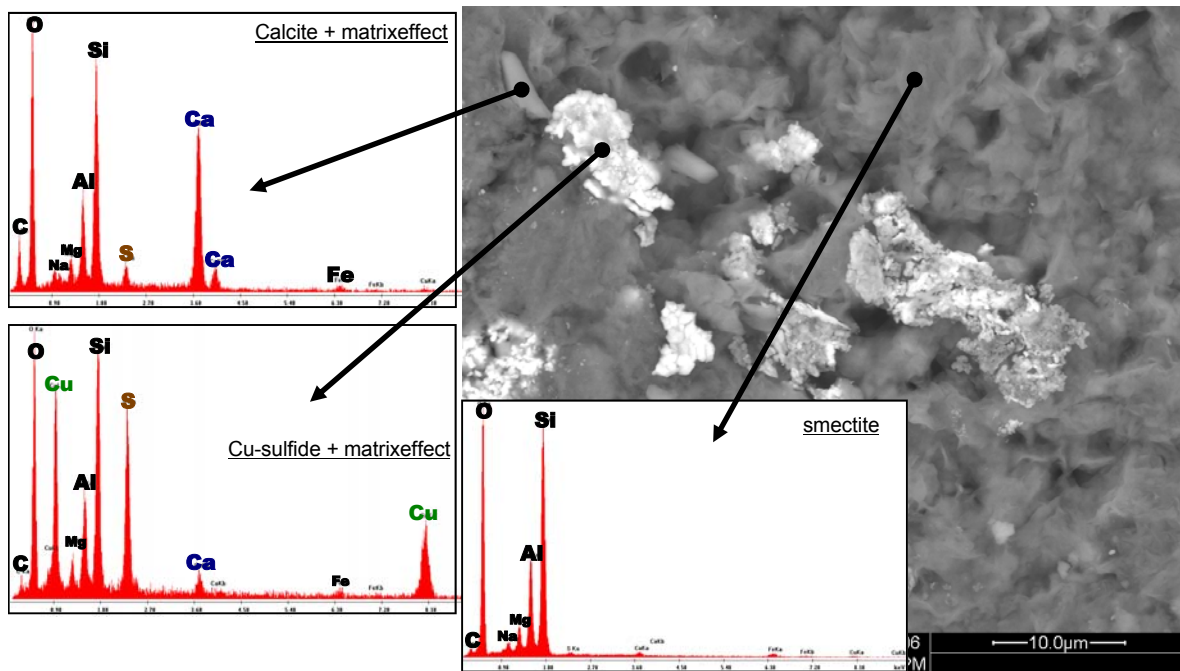


Figure 17: EDX investigation of the bentonite sample which was close to the Cu tube.

## Water uptake capacity

The water uptake capacity strongly depends on type and amount of exchangeable cation. Any collapse of the montmorillonite interlayer would result in a reduced water uptake capacity. Additionally, the pore system is believed to influence the water uptake capacity particularly at high relative humidity. Measuring the water uptake capacity, therefore, is a sensitive method for the determination of bentonite or clay alteration processes. The water uptake capacity of the LOT bentonite samples is shown in Figure 18.

Surprisingly, the samples which were close to the heater show a slightly higher water uptake capacity. This might be due to small differences of the cation occupation or changes of porosity. However, it is important to note, that the swelling ability, here determined by measuring the water uptake capacity, obviously was not affected by the extensive heating.

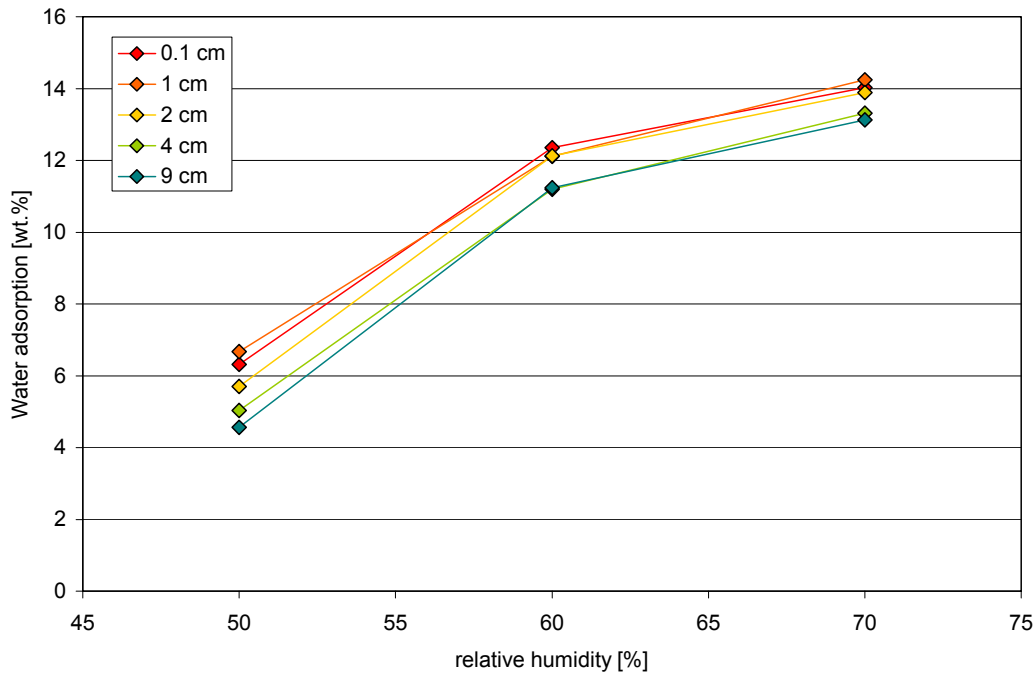


Figure 18: Water uptake capacity at 50, 60, and 70 % RH.

## Layer charge density (LCD)

For measuring the layer charge density with the whole set of alkylammonium chains the mass of material gained by sampling the A2 15 block was insufficient. Therefore, an additional block (A2 14N) was sampled and investigated by the alkylammonium method based on Lagaly (1994) and Olis et al. (1990). In the present study three different chain lengths of the alkylammonium ions were used ( $n_c = 11, 12, 13$ ).

Macroscopically, this second block revealed a higher gypsum concentration at the surface which has been in contact with the copper tube.

**Table 4: Comparison of the chemical composition of the second block (used for alkylammonium method) with the first block mainly considered in this study.**

	1 mm	1 mm	1 cm	1 cm	2 cm	2 cm	3 cm	3 cm	4 cm	4 cm	9 cm	9 cm	
	1 <sup>st</sup> block	2 <sup>nd</sup> block	1 <sup>st</sup> block	2 <sup>nd</sup> block	1 <sup>st</sup> block	2 <sup>nd</sup> block	1 <sup>st</sup> block	2 <sup>nd</sup> block	1 <sup>st</sup> block	2 <sup>nd</sup> block	1 <sup>st</sup> block	2 <sup>nd</sup> block	
SiO <sub>2</sub> [wt.-%]	68,3	67,7	68,3	68,4	68,3	68,3	no sample taken	68,0	67,7	67,5	68,4	68,4	
TiO <sub>2</sub> [wt.-%]	0,2	0,2	0,2	0,2	0,2	0,2		0,2	0,2	0,2	0,2	0,2	0,2
Al <sub>2</sub> O <sub>3</sub> [wt.-%]	20,7	20,6	20,8	20,7	20,7	20,7		20,5	20,5	20,4	20,7	20,7	20,7
Fe <sub>2</sub> O <sub>3</sub> [wt.-%]	3,9	3,9	4,0	4,0	4,0	4,0		4,0	4,0	3,9	4,0	4,0	4,0
MnO [wt.-%]	0,0	0,0	0,0	0,0	0,0	0,0		0,0	0,0	0,0	0,0	0,0	0,0
MgO [wt.-%]	3,0	2,9	2,7	2,6	2,7	2,6		2,6	2,5	2,4	2,4	2,4	2,4
CaO [wt.-%]	<b>1,2</b>	<b>1,5</b>	1,2	1,2	1,3	1,2		1,5	1,8	1,9	1,3	1,3	1,3
Na <sub>2</sub> O [wt.-%]	2,0	2,1	2,0	2,1	2,0	2,2		2,2	2,1	2,2	2,1	2,2	2,2
K <sub>2</sub> O [wt.-%]	0,5	0,5	0,5	0,6	0,5	0,6		0,6	0,5	0,6	0,5	0,6	0,6
P <sub>2</sub> O <sub>5</sub> [wt.-%]	0,1	0,1	0,1	0,0	0,0	0,0		0,0	0,0	0,0	0,1	0,1	0,1
(SO <sub>3</sub> ) [wt.-%]	0,2	0,5	0,2	0,2	0,3	0,2		0,3	0,7	0,7	0,3	0,2	0,2
(Cl) [wt.-%]	0,0	0,0	0,0	0,0	0,0	0,0		0,0	0,0	0,0	0,0	0,0	0,0
(F) [wt.-%]	<0,05	<0,05	<0,05	<0,05	<0,05	<0,05		0,00	<0,05	<0,05	0,06	0,06	0,06
Sum [wt.-%]	100,0	100,0	100,0	100,0	100,0	100,0	100,0	100,0	100,0	100,0	100,0	100,0	
LOI [wt.-%]	11,1	8,3	10,4	7,6	10,1	7,6	7,6	10,1	7,8	9,2	7,3	7,3	
(As)_SI [ppm]	13	12	14	9	11	12	9	11	9	13	12	12	
Ba_SI [ppm]	177	188	215	300	328	311	332	331	358	271	323	323	
Bi_SI [ppm]	<3	4	<3	4	<3	<3	4	<3	<3	<3	4	4	
Ce_SI [ppm]	104	111	112	109	111	112	114	116	122	116	99	99	
Co_SI [ppm]	<3	<3	<3	<3	<3	<3	<3	<3	<3	<3	<3	<3	
Cr_SI [ppm]	11	18	60	23	27	27	30	72	17	10	14	14	
Cs_SI [ppm]	<5	<5	<5	<5	<5	<5	<5	<5	<5	<5	<5	<5	
Cu_SI [ppm]	5764	5853	<b>4075</b>	<b>1053</b>	240	62	12	50	<10	<10	54	54	
Ga_SI [ppm]	26	27	27	28	27	30	29	27	29	28	28	28	
Hf_SI [ppm]	8	13	5	6	8	<5	5	7	8	7	<5	<5	
La_SI [ppm]	38	52	32	51	32	52	48	31	49	38	55	55	
Mo_SI [ppm]	27	27	6	4	<2	9	4	3	5	3	5	5	
Nb_SI [ppm]	27	28	26	30	27	27	29	30	28	27	28	28	
Nd_SI [ppm]	<50	<50	<50	51	55	57	55	<50	56	<50	66	66	
Ni_SI [ppm]	<b>&lt;3</b>	<b>1572</b>	5	409	<3	149	53	<3	24	<3	9	9	
Pb_SI [ppm]	27	24	32	38	44	48	49	46	45	42	44	44	
Rb_SI [ppm]	10	16	12	16	9	14	15	10	16	10	15	15	
Sb_SI [ppm]	<5	5	<5	<5	<5	<5	<5	5	<5	<5	<5	<5	
Sc_SI [ppm]	5	5	5	5	5	6	6	5	5	6	6	6	
Sm_SI [ppm]	<50	<50	<50	<50	<50	<50	<50	<50	<50	<50	<50	<50	
Sn_SI [ppm]	9	9	11	7	8	7	6	9	6	7	7	7	
Sr_SI [ppm]	213	202	220	221	233	230	279	301	353	215	224	224	
Ta_SI [ppm]	10	8	7	<5	<5	6	<5	7	<5	<5	<5	<5	
Th_SI [ppm]	45	40	41	39	43	41	40	41	40	43	40	40	
U_SI [ppm]	18	12	15	11	20	8	13	17	14	20	14	14	
V_SI [ppm]	9	<5	<5	7	<5	<5	<5	7	6	10	<5	<5	
W_SI [ppm]	<5	<5	<5	<5	<5	<5	<5	<5	<5	<5	<5	<5	
Y_SI [ppm]	37	43	39	42	39	43	42	37	40	38	41	41	
Zn_SI [ppm]	93	80	59	92	125	135	108	109	108	101	102	102	
Zr_SI [ppm]	179	188	184	194	175	190	191	181	184	181	195	195	

The comparability of both blocks was investigated by XRF:

- 1) The higher gypsum content at the bentonite tube contact surface is displayed by the CaO content (slightly higher in the 2<sup>nd</sup> block, sample 1 mm).

- 2) Slight deviations of the Cu content in samples 1 cm and 2 cm were found, which are likely due to small deviations of sampling distances.
- 3) Surprisingly, an elevated Ni content has been found in the second block. Here, a systematic difference between the first and the second block is evident. The Ni is supposed to stem from the cupro nickel shielding which surrounded the thermocouples (pers. comm. Karnland, 2007).

Overall, XRF strongly indicates the comparability of both blocks by considering the main element distribution, and in particular the distribution of 'structural elements' of smectites (such as Mg).

It is essential to note, that the LCD calculation from the  $d_{001}$  spacing is possible between the n-alkylammoniummono- and bilayer. The minimum d-spacing required is 13.7 Å. The MX 80 bentonite from the LOT test obviously contains low charged smectites. This is reflected by the low d-spacings of  $n_c = 11$  and 12. Only for  $n_c = 13$  a calculation of the LCD is reasonable. The differences are very small and vary between 13.8 and 13.8 Å.

Based only on the results presented in Table 5 it is impossible to determine an accurate mean value for the layer charge density. However, the following can be deduced:

- a) the LOT MX80 bentonite contains montmorillonites with a particularly low LCD. Three different MX80 samples which were investigated at BGR show higher LCD values.
- b) Despite the analytical problems caused by the low LCD it is impossible to unambiguously prove structural montmorillonite alteration because chain length 12 of the '1 mm sample' indicates a slight LCD increase whereas chain length 13 does not.

**Table 5:  $D_{001}$  spacing of three different n-alkylammonium-montmorillonites of the 6 samples and three reference MX80 samples. Calculation of LCD is only reasonable > 13.6 Å.**

sample	n = 11 d-value [Å]	LCD [eq/FU]	n = 12 d-value [Å]	LCD [eq/FU]	LCD (Olis et al., 1990) [eq/FU]	n = 13 d-value [Å]	LCD [eq/FU]
1 mm	13.5		14.1	0.28	0.26	13.8	0.23
1 cm	13.4		13.7	0.27	0.25	13.8	0.23
2 cm	13.4		13.6			13.7	0.23
3 cm	13.5		13.6			13.7	0.23
4 cm	13.6		13.9	0.27	0.25	13.8	0.23
9 cm	13.5		13.6			13.7	0.22
MX80 IB20 SKB	13.7	0.31	14.3	0.28	0.27	14.7	0.26
MX80 IB33 SC	13.8	0.31	14.3	0.28	0.27	14.7	0.26
MX80 GRS	13.4		13.5			14.6	0.25

The accuracy of the alkylammoniummethod is approximately  $\pm 0.01$  eq/FU. Therefore it has to be concluded that within this range no systematic dependency of LCD on the distances between the bentonite and the Cu tube could be identified.

## Magnetic fractionation

Magnetic fractionation was applied in order to obtain a sample with increased content of the Cu sulphide phase. The intention was to raise the concentration of this phase above the XRD detection limit in to get structural information about this phase. Accordingly, ca. 20 g of the first 2 cm of the second A2 block (A2 14N) were carefully broken and sieved. These different grain size fractions were subjected to a magnetic separator ('Franz Scheider') and analyzed by XRD, DTA, and IR. Surprisingly, in the magnetic 63 – 80  $\mu\text{m}$  fraction a high content of a hydrotalcite-group mineral could be identified by XRD (Figure 19). However, it remains unclear why this phase was enriched in the magnetic fraction.

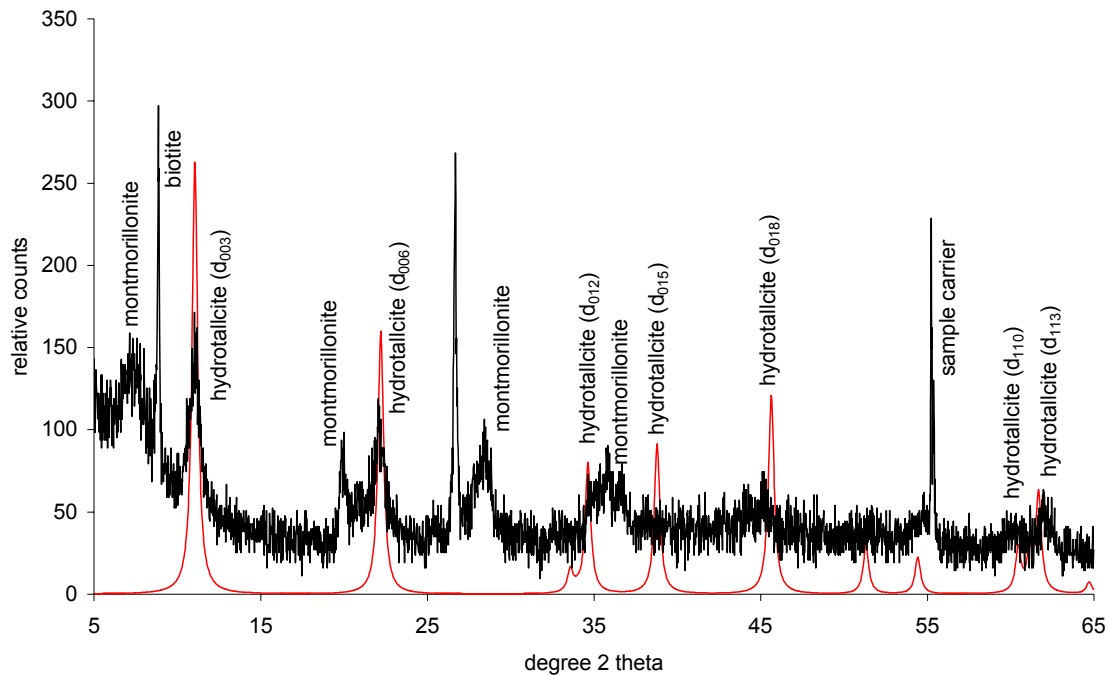


Figure 19: XRD pattern of the magnetic 63 – 80  $\mu\text{m}$  fraction compared to a hydrotalcite XRD pattern calculated according to Ennadi (2000).

## Summary and discussion

Chemical and mineralogical investigations of the LOT bentonite presented in this and other studies indicate that:

- a) gypsum redistributed by dissolution and precipitation,
- b) Cu was liberated from the tube and migrated into the bentonite, and
- c) no unambiguous evidence for structural alteration of the montmorillonite could be found.

All results being relevant with respect to the three main findings are summarized in Table 6.

**Table 6: Summary of analytical results being relevant with respect to the three main findings.**

Method/value	Figure / Table	Brief description of finding	Gypsum redistrib.	Cu corrosion	Structural alteration
1 XRF Al <sub>2</sub> O <sub>3</sub> , SiO <sub>2</sub>	Fig. 3	Minimum at 4 cm	??		
2 XRF Fe <sub>2</sub> O <sub>3</sub>	Fig. 4	No minimum	??		
3 XRF MgO	Fig. 4	Increase towards Cu tube			??
4 XRF CaO / SO <sub>3</sub>	Fig. 5	Maximum at 4 cm	+		
5 XRF Cu	Tab. 2	Increased Cu content until min. 4 cm		+	
6 XRF Mo	Tab. 2	Increased Mo content until 1 cm		+	
7 μ-EDXRF	Fig. 6	Increased Cu content until 2 cm		+	
8 XRD	Fig. 8	Gypsum peak only in 4 cm	+		no
9 CEC Ca <sup>2+</sup>	Fig. 9	Maximum at 4 cm	+		
10 CEC K <sup>+</sup>	Tab. 3	Slight increase towards Cu tube			??
11 CEC Mg <sup>2+</sup>	Fig. 9	Increase towards Cu tube			??
12 DTA MS 64	Fig. 11	Cu sulphide indicated		+	
13 MIR	Fig. 12	Gypsum band only in 4 cm	+		no
14 Light Microsc.	Fig. 15	bluish grains with metallic glance		+	
15 SEM EDX	Fig. 16, 17	Cu and S bearing grains		+	
16 H <sub>2</sub> O uptake cap.	Fig. 18	H <sub>2</sub> O uptake cap. not affected by heating			no
17 LCD AAM	Tab. 5	no systematic differences within range of precision			no
18 magnetic separation	Fig. 19 - 21	Hydrotalcite-group phase was found			??

a)

A variety of methods proved a gypsum peak at 4 cm. Since the gypsum distribution was homogenous at the beginning of the experiment it has to be concluded, that gypsum redistributed during the test period, most probably by dissolution and precipitation. From the first LOT sample which was considered in this study (except for LCD and magnetic fractionation) no sample was collected at 3 cm depth. Therefore, it was thought that the gypsum peak concentration at 4 cm likely represents the right shoulder of the peak at 3 cm of this study. The second LOT sample (considered for LCD and magnetic fractionation) revealed the gypsum peak at 4 cm (Table 4). However, the actual position of the gypsum peak concentration is less important for the understanding of corrosion and alteration processes. It is most important that its existence was proved unambiguously (even by different working groups). Both the Al<sub>2</sub>O<sub>3</sub> and the SiO<sub>2</sub> content as determined by XRF show a minimum at 4 cm which was interpreted as relative decrease caused by gypsum precipitation. However, it can not yet be explained why the other elemental concentrations do not reveal this minimum and if other Ca- and/or Mg- phases precipitated. We conclude that the actual mechanism for the redistribution of gypsum is not clear, yet.

b)

Cu corrosion led to the release of Cu from the tube which migrated into the bentonite block. XRF analysis, having the lowest Cu detection limit of the methods applied, proved an increased Cu concentration even in the '4 cm sample'. Surprisingly, Cu was not found in the interlayer of the montmorillonites. Instead, Cu sulphides could be found. Gypsum, a natural minor constituent of the bentonite (appr. 1.3 wt.%), is believed to be the S source, since it is the only S bearing mineral within the bentonite. It has to be concluded that sulphate, either from gypsum or from surrounding water, was reduced upon corrosion. A by-product of this reaction is  $\text{Ca}^{2+}$  which conceivably precipitates as carbonate together with  $\text{HCO}_3^-$  likely present in the surrounding water. This proposed corrosion mechanism is presented in Figure 20.

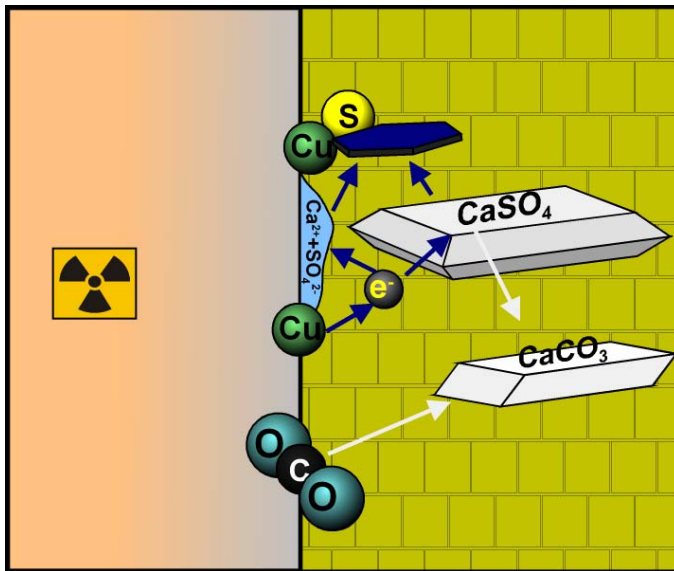


Figure 20: Sketch of model for corrosion mechanism (explanations are given in the text).

c)

XRF and CEC revealed a Mg increase nearby the Cu tube. The MgO increase as determined by XRF exceeds the MgO content as calculated from the increased CEC  $\text{Mg}^{2+}$  value appr. 5 times. This indicates, that the Mg peak cannot be explained by an increase in exchangeable  $\text{Mg}^{2+}$ , only. Accordingly, Mg either precipitated from pore water as hardly soluble phase (a higher solubility would have led to complete dissolution during the CEC experiment – XRF and CEC values would correspond to each other) or at least partly entered the montmorillonite structure. The latter possibility would have led to an increase of LCD which could not be detected neither by CEC nor AAM. Therefore, the Mg increase likely reflects the precipitation of Mg phases. It is at least conceivable that this phase is the hydrotalcite which was found by magnetic separation. The slight increase of exchangeable  $\text{Mg}^{2+}$ , in turn, indicates that this phase is partly soluble (keeping in mind the high liquid / solid ratio applied during the  $\text{BaCl}_2$  method). Yet, it could not be proved that the hydrotalcite was formed by alteration of the montmorillonite (e.g. beginning incongruent dissolution of edge octahedral sheets). Hence it cannot be concluded that it indicates structural alteration of the montmorillonite. Additionally, the slight increase of exchangeable  $\text{K}^+$  nearby the Cu tube is particularly interesting, because  $\text{K}^+$  adsorption is believed to

initiate illitization. Yet, no illitization (structural alteration of montmorillonite) could be detected.

It is worth mentioning that Plötze et al. (2007) reported a slight Mg increase in the bentonite nearby the heater of the Mont Terri heater project. Hence, it is at least conceivable that montmorillonites (in general) tend to release a small amount of Mg from octahedral sheet. From the results presented in the present study it is concluded that the Mg release of the LOT bentonite occurred to such a small extent that structural changes (e.g. change of layer charge density) could not be detected by IR, XRD, CEC and Alkylammoniummethod.

## Conclusions

In order to minimize mineral redistribution processes, which possibly lead to the formation of diffusion pathways, bentonites not containing relatively soluble minerals as calcite and gypsum should be used as geotechnical barrier material. Furthermore, the application of a bentonite not containing gypsum would lead to a reduction of the corrosion rate since the corrosion mechanism as observed is impossible without a S source.

The A3 parcel will be excavated after even longer time than the A2 parcel investigated in the present study. When the A3 parcel is analyzed, particular attention should be paid to K<sup>+</sup> fixation nearby the Cu tube as well as the formation of alteration products such as hydrotalcite.

## References

Dohrmann, R. (2006). Cation Exchange Capacity Methodology I: An Efficient Model for the Detection of Incorrect Cation Exchange Capacity and Exchangeable Cation Results. *Appl. Clay Science*, **34**, 31-37

Ennadi, A., Legrouri, A., De Roy, A., Besse, J.P. (2000). Shape and size determination for zinc-aluminium-chloride layered double hydroxide crystallites by analysis of X-ray diffraction line broadening. *J. Mater. Chem.*, **10**, p. 2337 – 2341.

Karnland, O., Sandén, T., Johannesson, L.-E., Eriksen, T., Jansson, M., Wold, S., Pedersen, K., Motamedi, M., Rosborg, B. (2000). Long term test of buffer material. Final Report on the pilot parcels. - SKB TR-00-22.

Karnland, O. (2007). pers. comm.

Maurel, C. (1964). *Bull. Soc. Franç. Minéral. Crist.*, **87**, p. 377.

Mehlich, A. (1948). Determination of cation- and anion-exchange properties of soils. *Soil Science* **66**, 429-445.

Lagaly, G. (1994). Layer charge determination by alkylammonium ions.- In: Mermut, A.R., editor: Layer charge characteristics of 2:1 silicate clay minerals, CMS Workshop Lectures Vol. 6, Boulder, CO, Clay Miner. Soc., p. 1 - 46.

Olis A.C., Malla P.B., Douglas L.A. (1990). The rapid estimation of the layer charge of 2:1 expanding clays from a single alkylammonium ion expansion.- Clay Min. 25, p. 39 - 50.

Plötze, M., Kahr, G., Dohrmann, R., Weber, H. (2007). Hydro-mechanical, geochemical and mineralogical characteristics of the bentonite buffer in a heater experiment. The HE-B project at the Mont Terri rock laboratory. Physics and Chemistry of the Earth, accepted for publication.